Circularly-Polarized Self-Homodyne Free-Space Optical Communication using Partial Stokes-Vector Receiver

Shota Ishimura[1], Hidenori Takahashi[1], Go Soma[2], Kento Komatsu[2], Takuo Tanemura[2], Takehiro Tsuritani[1], and Masatoshi Suzuki[1]
[1]KDDI Research Inc., 2-1-15 Ohara, Fujimino-shi, Saitama, 356-8502, Japan
[2]School of Engineering, The University of Tokyo, 7-3-1 Hongo, Bunkyo-ku, Tokyo 113-8656, Japan
sh-ishimura@kddi.com

Abstract: We propose a circularly-polarized self-homodyne free-space optical (FSO) system using a partial Stokes-vector receiver (SVR) that enables polarization rotation-independent coherent signal reception. The advantage over the standard SVR is verified through a 100-Gbps FSO experiment.

1. Introduction

Self-homodyne transmission systems have recently attracted significant attention due to their simpler system configurations than the conventional full coherent systems. Since a single laser source is shared between signal and local oscillator (LO) components, they should have ideally the same wavelength and phase noise. Consequently, self-homodyne systems enable uncooled operation and potentially eliminate the need for or lighten the carrier-phase estimation (CPE) process. These benefits have been experimentally confirmed via considerable fiber transmission experiments [1-8]. However, the need for polarization tracking mechanisms in either the optical [1,2] or electrical domain [4-8] is still the remaining issue. In fact, optical polarization tracking requires adaptive polarization control at the device level. Polarization rotation can also be compensated in the electrical domain if signal and LO components are polarization-multiplexed together and detected by a Stokes-vector receiver (SVR), which outputs 3-dimensional (3D) signals, i.e., the Stokes parameters of S_1, S_2, and S_3 (Fig. 1a) [6-8]. However, such 3D signal detection also increases hardware complexity.

While these issues are inevitable in fiber-optic communications, there is a potential to completely avoid them if we apply self-homodyne systems to free-space optical (FSO) communications, especially in space where there exists no birefringence and consequently polarization states can be completely fixed. Even in this case, however, it is difficult to align a transmitter polarization axis to a receiver one due to the ever-changing angles of rotating satellites. Therefore, circular polarization has been employed in commercial wireless applications such as GPS systems [9] and 4K/8K satellite broadcasting [10] and was also considered in optical satellite communications [11-13]. This is because circular polarization states never change in space regardless of receiving angles and thus never suffer from the vertical/horizontal alignment.

In this paper, we propose a circularly-polarized self-homodyne FSO system using a partial SVR. We assign signal and LO components to right(left)- and left(right)-handed circular polarization states, respectively (Fig. 1b). In contrast to the conventional circular-polarization shift-keying (CPolSK) format that only exploits a 1D constellation space [12,13], the in-phase and quadrature (IQ) components of the signal can immediately be retrieved from part of the Stokes parameters, S_1 and S_2, without any polarization tracking mechanisms due to the fixed circular polarization states. Its advantage over the standard SVR was experimentally verified, and we achieved a gross rate of 100 Gbps using the circular polarization system. Since self-homodyne detection itself has significant advantages in space such

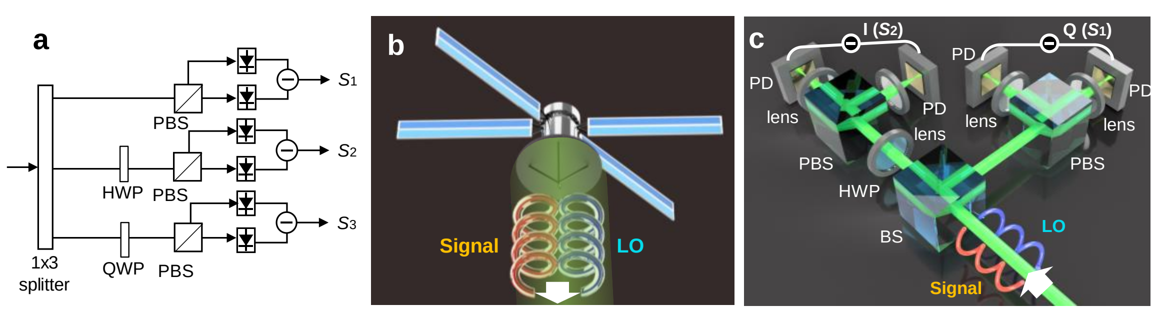

Fig. 1: a conventional standard SVR system. **b** illustration of circularly-polarized signal and LO waves emitted from a rotating satellite. **c** partial SVR enabling the IQ retrieval of the circularly-polarized self-homodyne signals.

as its robustness against the Doppler shift, we believe that the use of circular polarization incorporated in self-homodyne systems opens new possibilities in FSO communications.

2. Working principle

We here quantitatively explain the concept. First, we define the Stokes parameters as $S_1 = |E_x|^2 - |E_y|^2$, $S_2 = 2\,\mathrm{Re}[E_x E_y^*]$, and $S_3 = 2\,\mathrm{Im}[E_x E_y^*]$, where E_x and E_y are the components of a Jones vector in an *x* (or *y*) linear polarization basis on the transmitter side. Also, let the complex amplitudes of signal and LO components be E_{sig} and E_{LO}, respectively. Therefore, the Jones vector on the transmitter side, J, is given as $J = E_{sig}(1 \quad j)^T/\sqrt{2} + E_{LO}(1 \quad -j)^T/\sqrt{2}$, where T stands for transpose. Then, the Jones vector, J', rotated by the angle of θ with respect to the *x*-axis on the receiver side, is given as:

$$J' = \begin{pmatrix} E_x' \\ E_y' \end{pmatrix} = \begin{pmatrix} \cos\theta & \sin\theta \\ -\sin\theta & \cos\theta \end{pmatrix} \left\{ \frac{E_{sig}}{\sqrt{2}} \begin{pmatrix} 1 \\ j \end{pmatrix} + \frac{E_{LO}}{\sqrt{2}} \begin{pmatrix} 1 \\ -j \end{pmatrix} \right\} = e^{j\theta} \frac{E_{sig}}{\sqrt{2}} \begin{pmatrix} 1 \\ j \end{pmatrix} + e^{-j\theta} \frac{E_{LO}}{\sqrt{2}} \begin{pmatrix} 1 \\ -j \end{pmatrix}. \tag{1}$$

It is worth noting that the angle just affects the absolute phases and does not change each circular polarization state. By substituting Eq. (1) into the definition of the Stokes parameters, we obtain:

$$S_1' = 2\,\mathrm{Re}[e^{j2\theta} E_{sig} E_{LO}^*] \quad (2), \qquad S_2' = -2\,\mathrm{Im}[e^{j2\theta} E_{sig} E_{LO}^*] \quad (3), \qquad S_3' = -(|E_{sig}|^2 - |E_{LO}|^2). \quad (4)$$

It is found from the above equations that the desired signal-to-LO beat term, i.e., the IQ component of the signal can be completely retrieved from $S_1' + jS_2'$ even in the presence of the angle rotation although it includes the additional phase shift of 2θ. However, such a phase rotation has no impact on performance since it is completely removed with laser phase noise in the standard CPE process. In addition, since the S_3' parameter, which denotes the power difference of the right- and left-handed circularly-polarized lights is not necessary for the IQ retrieval, we can definitively obtain the receiver configuration by eliminating the branch as shown in Fig. 1c. We should emphasize that the branch elimination reduces the internal receiver loss and thus improves the receiver sensitivity by 1.76 dB compared to the standard SVR [14].

The aforementioned concept can also be graphically understood in the Stokes space. Figures 2a and 2b show the 3D constellation plot of the conventional self-homodyne 16QAM signal (the powers of the signal and LO are assumed to be equal), and its projection onto the S_2 - S_3 plane, respectively. However, if there is an angle rotation, as shown in Fig. 2c (this shows an example case of 45-deg. rotation), the projection no longer reflects the original constellation, as shown in Fig. 2d. On the other hand, Figures 2e and 2f show the 3D plot and the corresponding projection on the S_1 - S_2 plane of the circularly-polarized self-homodyne 16QAM signal. Even if there is a 45-deg. rotation in this case, the projection remains the same as shown in Fig. 2h. This is because the angle mismatch just rotates the Stokes vector around the S_3 axis and thus has no impact on the projection on the S_1 - S_2 plane except for the phase shift of 2θ.

3. Experiments

We conducted a proof-of-concept experiment. The experimental setup is shown in Fig. 3. On the transmitter side, a continuous-wave (CW) light source was generated from a laser diode (LD), the linewidth of which was ~ 100 kHz. Then, the light was split using a polarization-maintaining (PM) coupler, and one of them was injected into an IQ modulator (IQM) which was driven by an arbitrary waveform generator (AWG) running at 120 GS/s. By using offline digital signal processing (DSP), we first generated 10-Gbaud QPSK signals, filtered them using a raised-cosine filter

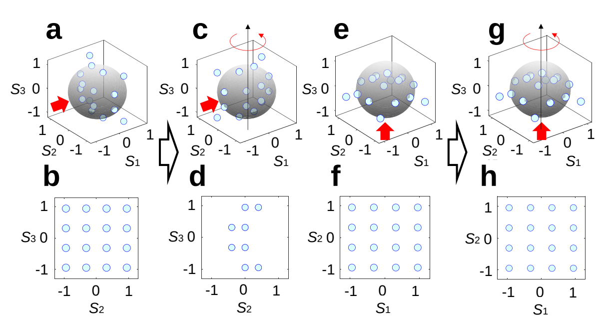

Fig. 2: 3D plots in the Stokes space and 2D projections.

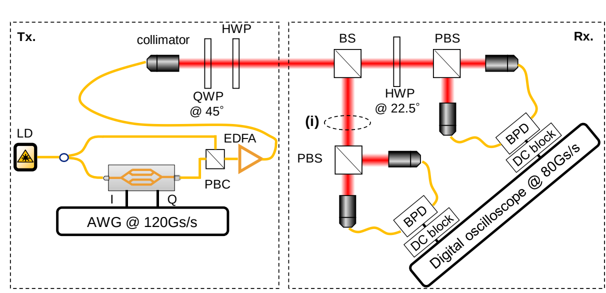

Fig. 3: Experimental setup.

with a roll-off factor of 1, and loaded them to the AWG. The modulated light was polarization-multiplexed with the other unmodulated path using a polarization-beam combiner (PBC). Subsequently, they were amplified using a PM erbium-doped fiber amplifier (EDFA) and guided to a collimator. The collimated beam was passed through a quarter-wave plate (QWP) tilted by 45 deg. to convert the x(y)-polarization basis to the circular polarization basis. The transmitted circularly-polarized beam was then received using a partial SVR. At the partial SVR, the signal was first split by a beam splitter (BS), and one of them was directly guided to a polarization-beam splitter (PBS). The two outputs from the PBS were detected using a balanced PD (BPD) and the electrical output was captured by a digital oscilloscope running at 80 GS/s. On the other hand, the other path split from the BS passed through a half-wave plate (HWP) tilted by 22.5-deg. and guided to another PBS. As with the other branch, the outputs were detected using another BPD and its electrical output was captured by another port of the oscilloscope. Finally, the signal was equalized using the decision-directed least-mean-square (DD-LMS) algorithm at offline DSP.

We first show the performance independence of the circularly-polarized self-homodyne system on angle rotation using error-vector magnitudes (EVMs). In order to emulate angle rotation, we inserted an HWP just after the QWP on the transmitter side and rotated it manually. For comparison, we also measured EVMs when using the standard linear-polarization-based SVR. In this case, the QWP was removed from the transmitter, and it was instead inserted in the place labeled as (i) on the receiver side, as shown in Fig. 3 so that the receiver could detect the S_2 and S_3 components. Figure 4a shows the results. As shown there, the EVMs were maintained at ~9% regardless of rotation angles when using the circularly-polarized self-homodyne system, while they significantly deteriorated, especially at angles of 20 and 70 degrees when using the conventional SVR. This is because the maximum crosstalk between the x- and y-polarizations occurs when the HWP angles are 22.5 and 67.5 degrees, as shown in Fig. 2d. Finally, we demonstrated a high-speed experiment. We increased the baud rate to 25 Gbaud and changed the modulation format to 16QAM. In addition, the HWP angle was set at 22.5 deg., which was the worst case for the standard SVR system. Figure 4b shows the constellation of the 16QAM signal. As shown there, the IQ signal was successfully retrieved, and the corresponding EVM and BER were measured to be 12.6% and 2.1×10^{-4}, respectively, which is below the threshold of the 7% hard-decision (HD) forward-error-correcting (FEC) code. Therefore, we achieved a gross rate of 100 Gbps and a net rate of 93.4 Gbps. Note that these rates are limited due to the imperfection of the homemade receiver such as power imbalance and path length mismatch. However, we believe that they can be increased further by elaborating the receiver. It should also be noted that the current bulky space-optic components of the receiver should readily be replaced with a thin dielectric metasurface and could be more compact for practical use [15].

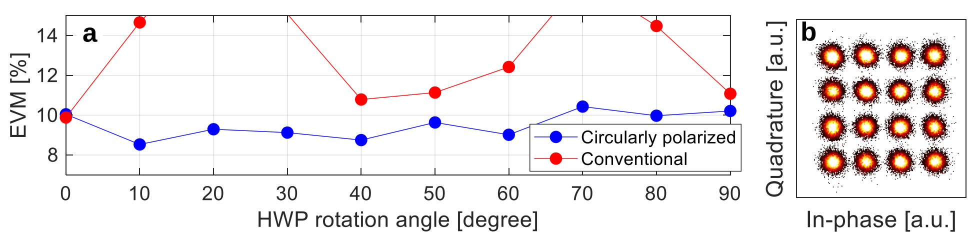

Fig. 4: a EVM dependence on angle rotation. **b** constellation plot of 25-Gbaud 16QAM.

4. Conclusion

We have proposed a circularly-polarized self-homodyne FSO system using a partial SVR that enables polarization rotation-independent coherent signal reception. The independence of the circularly-polarized system on rotation angle was experimentally verified. Also, we successfully demonstrated signal reception of a 16QAM signal via an FSO experiment with a gross rate of 100 Gbps.

Acknowledgment

This work contains the results obtained from the commissioned research 03601 by the National Institute of Information and Communications Technology (NICT), Japan.

5. References

[1]. T. Gui *et al.*, *OFC*2020, Th4C.3 (2020).
[2]. L. Wang *et al.*, *OFC*2021, M5G.3 (2021).
[3]. R. Zhang *et al.*, *OFC*2022, W1G.1 (2022).
[4]. R. S. Luís *et al.*, *ECOC*2015, Tu.3.4.7 (2015).
[5]. B. Boriboon *et al.*, *ECOC*2022, Th3A.2 (2022).
[6]. D. Che *et al.*, *J. Light. Technol.* **33**, 678-684 (2015).
[7]. S. Ishimura *et al.*, *J. Light. Technol.* **39**, 6150-6158 (2021).
[8]. S. Ishimura *et al.*, *OFC*2022, M4J.6 (2022).
[9]. D. M. Pozar *et al.*, *IEEE Trans. Antennas Propag.* **45**, 1618-1625 (1997).
[10]. ITU-R BT.2485-1 (2022).
[11]. T. Kuri *et al.*, *GLOBECOM* '95 **3**, 2003-2007 (1995).
[12]. S. Á. Jaramillo Flñrez, *IEEE Latin-American Conference on Communications*, 1-6 (2010).
[13]. X. Zhao *et al.*, *J. Opt. Commun. Netw.* **1**, 307-312 (2009).
[14]. T. Tanemura *et al.*, *J. Light. Technol.* **38**, 447-456 (2019).
[15]. G. Soma *et al.*, *Optica* **10**, 604-611 (2023).